ELSEVIER

Chemical Engineering Journal 137 (2008) 14–22

Chemical Engineering Journal

www.elsevier.com/locate/cej

Calcium carbonate microcapsules encapsulating biomacromolecules

Masahiro Fujiwara [a,*], Kumi Shiokawa [a,1], Kenichi Morigaki [a,1], Yingchun Zhu [b], Yoshiko Nakahara [a,1]

[a] *National Institute of Advanced Industrial Science and Technology (AIST), Kansai Center, 1-8-31 Midorigaoka, Ikeda, Osaka 563-8577, Japan*
[b] *Shanghai Institute of Ceramics, Chinese Academy of Sciences, 1295 Ding Xi Road, Shanghai 200050, China*

Received 14 May 2007; received in revised form 4 July 2007; accepted 6 September 2007

Abstract

This paper reports the preparation of $CaCO_3$ microcapsules and the direct encapsulation of biomacromolecules such as bovine serum albumin (BSA) and duplex DNA into the $CaCO_3$ microcapsules. Vacant $CaCO_3$ microcapsules were effectively obtained by interfacial reaction method using carbonate salts and calcium salts, which were dissolved in inner water phase or outer one, respectively. For the fabrication of microcapsule structure, the formation of vaterite as a metastable phase of calcium carbonate crystal was an important factor. When some biomacromolecules were dissolved in the aqueous solution of $(NH_4)_2CO_3$ as the inner water phase, these macromolecules were successfully encapsulated into $CaCO_3$ microcapsules. Biomacromolecules included in the microcapsules scarcely eliminated without the fracture of the microcapsule particles. These properties of encapsulated biomacromolecules might be utilized in various bio-related materials.

Keywords: Microcapsule; Bioencapsulation; Calcium carbonate; Emulsion; Protein; DNA; Inorganic–organic composite material

1. Introduction

Small particles are potent materials in the fields of biotechnology and bio-nanotechnology [1–7]. When these particles penetrate into the living body, they will play various roles in biomedical and clinical applications. Recently inorganic spherical particles in micro- and nano-size are actively prepared by various methods for the applications to biomedical uses [8–11]. Silica particles are the most representative inorganic substance of these applications [12–14]. We also published the preparations of silica microcapsules [15] and the direct encapsulation of biomacromolecules into them [16] by interfacial reaction method using W/O/W emulsion. However, the degradability of silica within the living body is thought to be poor and the body residue of silica might become some serious problems [17–19], although some recent reports revealed the comparatively high biocompatibility of silica nanoparticles [20–22]. Biodegradable components are predominant options of clinical and biomedical applications not only in organic polymer materials but also in porous inorganic ones. Calcium phosphates [23–25] are typical biodegradable and biocompatible inorganic materials. These inorganic components will provide lower-risk materials in various practical applications. Recently we also reported a simple method to prepare calcium phosphate particles including biomacromolecules [26]. Although no hollow structure was formed in this case, biomacromolecules such as BSA and duplex DNA were successfully introduced into the crystalline matrices of calcium phosphates such as hydroxyapatite. The preparation of hollow calcium phosphates is still under investigation in our research group.

We have already succeeded the preparation of calcium carbonate ($CaCO_3$) microcapsules (spherical hollow particles) by the interfacial reaction method [27]. $CaCO_3$ is also a biocompatible and biodegradable inorganic material. Many materials chemists examined a number of new fabrication procedures, a part of which are linked to biomineralization research [28]. The preparation of hollow $CaCO_3$ particles is also a current active field of materials chemistry [29–33]. Furthermore, the utilization of porous $CaCO_3$ (but not hollow structure) to biomedical applications is a recent topic of inorganic materials science [34–36]. We found recently that $CaCO_3$ hollow microcapsules

* Corresponding author. Tel.: +81 72 751 9253; fax: +81 72 751 9628.
E-mail address: m-fujiwara@aist.go.jp (M. Fujiwara).
[1] Tel.: +81 72 751 9253; fax: +81 72 751 9628.

1385-8947/$ – see front matter © 2007 Elsevier B.V. All rights reserved.
doi:10.1016/j.cej.2007.09.010

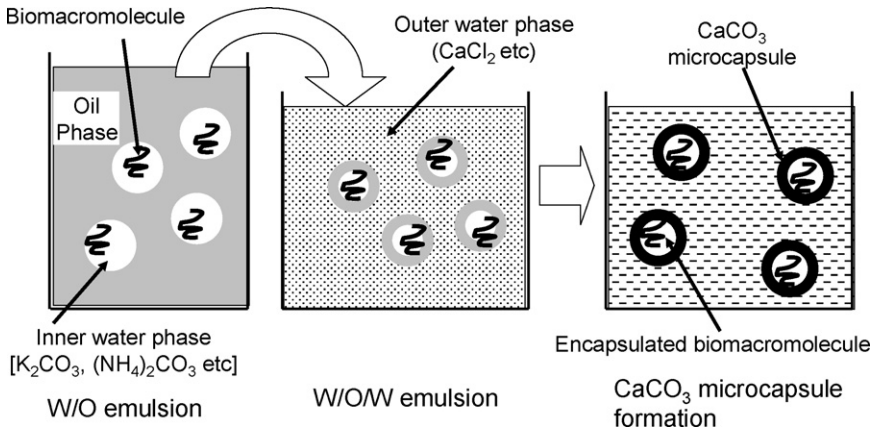

Fig. 1. A systematic scheme of the preparation of $CaCO_3$ microcapsule encapsulating biomacromolecules.

encapsulating biomacromolecules were produced by the analogous methods to silica microcapsules. This paper reports our latest results of the direct encapsulation of biomacromolecules into $CaCO_3$ microcapsules as shown in Fig. 1. The methods and the manners of the encapsulation of biomacromolecules are described in detail.

2. Materials and methods

2.1. Chemicals

All chemicals used in this paper were commercial available and were used without further purification. BSA [albumin from bovine serum (Cohn Fraction V, pH 7.0)], papain, lysozyme (lysozyme from egg white) and deoxyribonucleic acid sodium salt from salmon spermary powder (300–9000 kDa, 460–14,000 bp) were obtained from Wako Pure Chemical Industries. Ovalbumin was purchased from Sigma as albumin from chicken egg white, grade V.

2.2. Procedures

2.2.1. Vacant $CaCO_3$ microcapsules

Vacant $CaCO_3$ microcapsules were obtained by our described procedure using the interfacial reaction method [27]. A typical preparation procedure is described as follows. An aqueous solution (32 mL) of K_2CO_3 (13.27 g, 96.0 mmol) as the inner water phase of Fig. 1 was mixed with the homogenizing *n*-hexane solution (48 mL) of Tween 80 (0.67 g) and Span 80 (0.33 g). After emulsifying at about 8200 rpm for 1 min (Heidolph DIAX 900), the resulting solution was poured quickly into the aqueous solution (640 mL) of $CaCl_2{\cdot}2H_2O$ (28.23 g, 192 mmol) as the outer water phase with mechanical stirring at 400 rpm. After mixing this resulting solution for 10 min, the solid was filtered, washed with fresh deionized water three times (500 mL each) and 100 mL of methanol one time. Finally the solid was dried at 100 °C for sufficient periods (generally more than 12 h). The weights of vacant samples obtained by this procedure were generally from 8 to 10 g. A $CaCO_3$ sample by simple mixing was obtained from the same aqueous solutions as the interfacial reaction method without using *n*-hexane solution (with mechanical stirring at 400 rpm). After 10 min stirring, the resulting solid was filtered and the following procedures were similar to above.

2.2.2. $CaCO_3$ microcapsules encapsulating biomacromolecules

$CaCO_3$ microcapsules encapsulating biomacromolecules were obtained by an analogous method to silica microcapsule [16]. As most biomacromolecules seems to be denatured or decomposed in the high alkaline solution of K_2CO_3, $(NH_4)_2CO_3$ was employed instead of K_2CO_3 in the cases of biomacromolecule encapsulation. An aqueous solution dissolving a prescribed amount of a biomacromolecule shown in Table 2 was mixed with an aqueous solution of $(NH_4)_2CO_3$ (9.22 g, 96.0 mmol). The total volume of the solution was fixed to 32 mL. This solution was used for the preparation as the internal water phase. The following treatments were similar to the vacant $CaCO_3$ microcapsule as mentioned above. The drying of the samples was performed at room temperature.

2.3. Analysis

X-ray diffraction patterns were recorded using Mac Science MXP3V diffraction meter with Ni filtered Cu Kα radiation ($\lambda = 0.15406$ nm) using common glass plates. Scanning electron microscopy (SEM) images were measured using JEOL JSM-5200 microscope apparatus. In transmission electron microscope (TEM) observation, the materials were characterized by field emission transmission electron microscopy (FETEM) recorded on a JEOL JEM-2100F using an accelerating voltage of 200 kV. Diffuse reflectance UV spectra were obtained with a JASCO V-550 spectrometer equipped with an integrating sphere. Kubelka–Munk functions were plotted versus the wavelength. UV spectrum measurement of aqueous solutions was performed using JASCO V-530 spectrometer by a common procedure. Thermogravimetric analyses (TGA) were performed using by Shimadzu TGA-50 apparatus. All samples were held in a platinum sample holder and were heated under air at the rate of 5 °C/min. Nitrogen adsorption–desorption isotherms were obtained at −196 °C (in liquid N_2) using a Bellsorp Mini instrument (BEL JAPAN, Inc.). Outgassing was performed under dry nitrogen flow at 100 °C over 12 h. BJH calculation was per-

Table 1
Porosity and particle size profiles of $CaCO_3$ microcapsules

Sample	IWP	OWP	Specific surface area (m^2/g)[a]	Pore volume (mL/g)[b]
VC–K–Cl	K_2CO_3	$CaCl_2$	2.39	0.036
VC–NH–Cl	$(NH_4)_2CO_3$	$CaCl_2$	6.06	0.093
VC–NH–OAc	$(NH_4)_2CO_3$	$Ca(OAc)_2$	18.43	0.206
VC–Cl–K	$CaCl_2$	K_2CO_3	7.48	0.085
VC–OAc–K	$Ca(OAc)_2$	K_2CO_3	2.28	0.052
Calcite	[c]		0.423	<0.01

[a] BET specific surface area.
[b] Pore volumes are estimated from the adsorption branches of nitrogen sorption isotherms.
[c] Commercial calcite $CaCO_3$ powder.

formed to estimate the mesopore size using adsorption branches of isotherms.

Fluorescence microscopy observation was performed using an Olympus BX51WI fluorescence microscope [Uplan S Apo (X100); 1.40NA]. In the case of BSA encapsulating microcapsules, an aqueous solution of BSA with 1% of BSA bearing fluorescent substance (albumin, fluorescein isothiocyanate conjugate bovine from Sigma) was used for the preparation [16]. Samples were observed with excitation light by the OLYMPUS U-MNIBA2 filter set (excitation: 470–490 nm, emission: 510–550 nm). In the case of DNA, ethidium bromide (10 mg/mL aqueous solution) was impregnated to made-up $CaCO_3$ microcapsules encapsulating duplex DNA. This sample was observed by the OLYMPUS U-MNUA2 filter set (excitation: 369–370 nm; emission: 420–460 nm). Before observation, these samples were thoroughly washed with deionized water.

3. Results and discussion

3.1. Preparation of vacant $CaCO_3$ microcapsules

The preparation of $CaCO_3$ microcapsules has been already reported briefly in our previous paper [27]. In this paper, we wish to show the details of these materials, which were not mentioned before. The texture properties of vacant $CaCO_3$ microcapsules prepared in this study are listed in Table 1. The sample names are assigned with the counter ions of carbonate and calcium ions of material sources. For example, a $CaCO_3$ microcapsule obtained from K_2CO_3 and $CaCl_2$ was named as VC–K–Cl, where VC means "vacant $CaCO_3$". The SEM image of a typical $CaCO_3$ microcapsule obtained from K_2CO_3 and $CaCl_2$ is shown in Fig. 2(A). The spherical particles were clearly observed. In Fig. 3(A) and (B), the TEM images of this microcapsule are displayed. These TEM images suggested that these particles are hollow. The inside parts of the particles are likely to be lighter than the outside, although no clear line often observed in hollow particles [32] was not detected. It is thought that the density inside of this $CaCO_3$ particle is lower than that of surface (shell) part. We attempted to produce partially broken $CaCO_3$ microcapsule, which is suitable for observing shell and hollow structure. However, $CaCO_3$ microcapsule was hard solids and shattered even by careful crashing. We did not succeed the observation of hollow structure by SEM image. As comparison, TEM images of $CaCO_3$ particles obtained by a simple mixing method (not interfacial reaction method) are also shown in Fig. 3(C) and (D). In these non-hollow $CaCO_3$ particles, no contrast of images was observed in between inside and outside of the particles. Therefore, the interfacial reaction method using W/O/W emulsion is considered to produce hollow $CaCO_3$ spherical particles (microcapsules) similar to silica [15]. The main crystalline phase of this $CaCO_3$ material was vaterite that is a metastable phase of crystalline $CaCO_3$. The XRD pattern of this $CaCO_3$ is shown in Fig. 4. Although some peaks of calcite phase of $CaCO_3$ such as the sharp peak at about 29.5 in 2θ (a typical XRD pattern of calcite is also illustrated as C in Fig. 4) were found in the XRD pattern, main peaks detected in the pattern A of Fig. 4

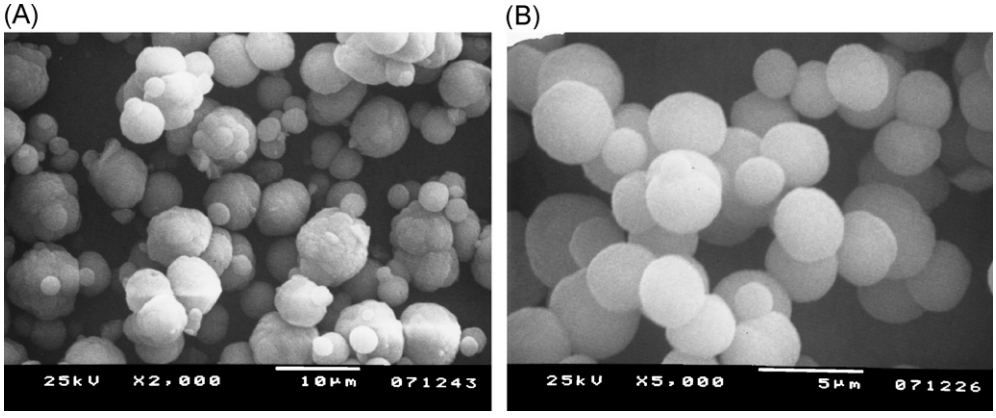

Fig. 2. (A) A SEM image of $CaCO_3$ microcapsule obtained from K_2CO_3 and $CaCl_2$ (VC–K–Cl). (B) A SEM image of $CaCO_3$ microcapsule obtained from $(NH_4)_2CO_3$ and $CaCl_2$ (VC–NH–Cl).

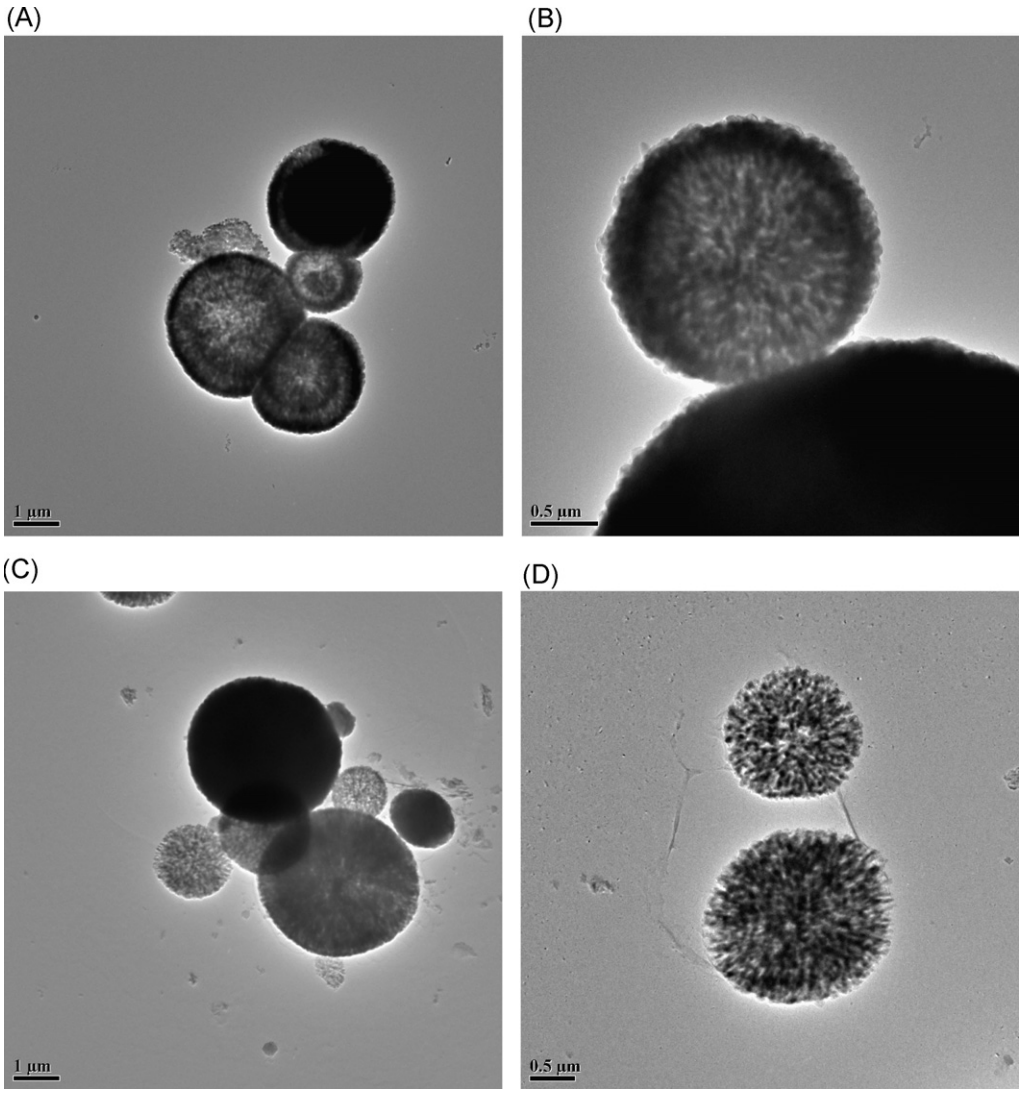

Fig. 3. (A and B) TEM images of $CaCO_3$ microcapsule obtained from K_2CO_3 and $CaCl_2$ (VC–K–Cl). (C and D) TEM images of $CaCO_3$ obtained by simple mixing of K_2CO_3 and $CaCl_2$.

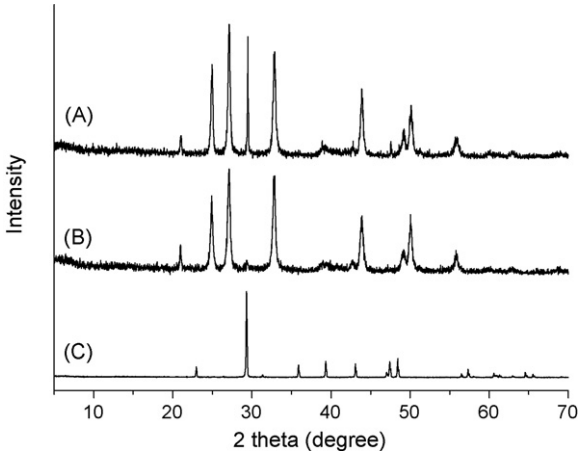

Fig. 4. X-ray diffraction patterns of $CaCO_3$ microcapsules. (A) VC–K–Cl and (B) VC–NH–Cl. (C) Calcite $CaCO_3$.

were vaterite. We separated the microcapsules from the mixed reaction solution just after 10 min by filtration. When the microcapsules were aged in the reacted solution for longer time, the peaks of calcite phase increased with time in XRD pattern. Some rhombic particles were also found with spherical microcapsules in this case. It is known that the shape of calcite and vaterite are rhombic and spherical, respectively. The rhombic particles formed in longer aging must be calcite $CaCO_3$ transformed from vaterite. The $CaCO_3$ particles by the simple mixing method were also spherical as shown in Fig. 3(C) and (D). These particles also mainly consisted of vaterite $CaCO_3$ with some calcite phase confirmed by XRD patterns (not shown). As this particle was filtrated just after 10 min, the transformation of vaterite to calcite was considerably restricted to afford the mixed phase. The $CaCO_3$ microcapsules are obtained only when vaterite phase of $CaCO_3$ formed the shell part of microcapsules.

Some other carbonate and calcium salts were also applicable for this preparation as summarized in Table 1. For example, $(NH_4)_2CO_3$ could be used instead of K_2CO_3 and the SEM image

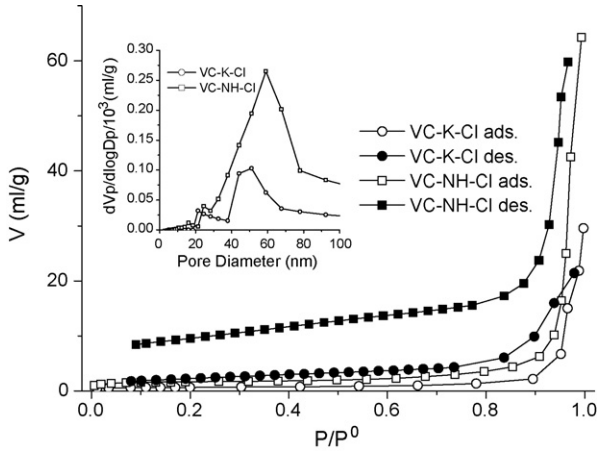

Fig. 5. Nitrogen adsorption–desorption isotherms of $CaCO_3$ microcapsules, VC–K–Cl and VC–NH–Cl. The BJH pore size distributions of VC–K–Cl and VC–NH–Cl estimated by the desorption branches of the isotherms are illustrated in the inset.

of this $CaCO_3$ microcapsule is shown in Fig. 2(B). Smaller particles than $CaCO_3$ microcapsule obtained from K_2CO_3 were obtained. We reported before that the fast formation of precipitate reduces the particle size of silica microcapsules [15]. It is thought that the solution of $(NH_4)_2CO_3$ (pH ~9.5) becomes acidity with $CaCl_2$ solution to produce $CaCO_3$ precipitate more quickly than that of K_2CO_3, (pH > 13), because of less basicity of the solution of $(NH_4)_2CO_3$. Therefore, the particles size of $CaCO_3$ microcapsules using $(NH_4)_2CO_3$ became smaller than that using K_2CO_3. In the XRD pattern of this microcapsule, the peak from calcite phase of $CaCO_3$ was scarcely detected to indicate that this microcapsule was exclusively composed of vaterite phase. Table 1 summarizes the data of specific surface area and pore volume of various $CaCO_3$ microcapsules prepared from various solutions. As $CaCO_3$ generally has low surface area, some modified methods have been attempted to produce porous $CaCO_3$ particles for biomedical applications [34–36]. A commercially available $CaCO_3$ as calcite had a poor surface area as shown in Table 1, while $CaCO_3$ microcapsules obtained by interfacial reaction method had higher surface areas. The reported porous calcite $CaCO_3$ particles have approximately 8.8 m^2/g of specific surface area [36]. $CaCO_3$ microcapsules we prepared here had the high surface areas comparative with those reported ones [36]. The pore volumes of these $CaCO_3$ microcapsules were also higher than the common calcite $CaCO_3$, and nearly equal to the reported porous $CaCO_3$ particles [36]. Two representative nitrogen adsorption-desorption isotherms are shown in Fig. 5. The peak pore diameters of these two samples were observed in from 50 to 60 nm. Comparatively large mesopores were formed in the shells of the $CaCO_3$ microcapsules. The same kind of adsorption hysteresis was obviously found in both isotherms. This hysteresis pattern is regarded as type H1 of IUPAC classification, which is often observed in aggregated materials of uniform spherical particles [37]. A TEM image of a $CaCO_3$ microcapsule at high magnification in Fig. 6 showed that these mesopores were formed as the spaces between small $CaCO_3$ crystal particles. The distances between the small crystals were approximately from 50 to 80 nm. For example, the length of the

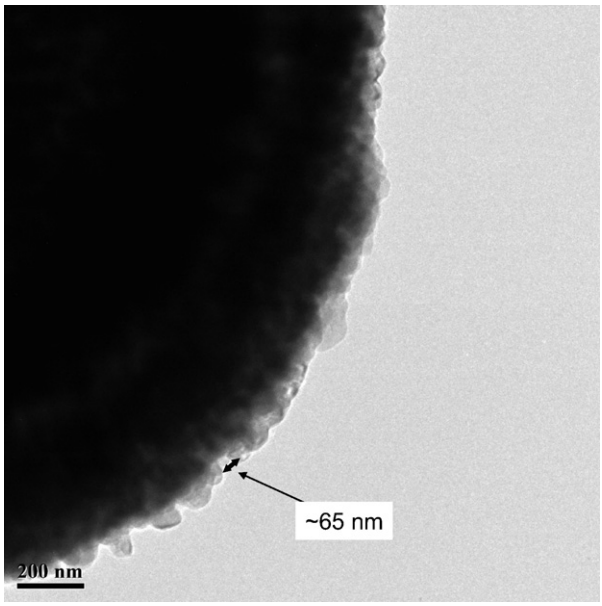

Fig. 6. TEM image of $CaCO_3$ microcapsule (VC–K–Cl) at high magnification.

two-headed arrow in Fig. 6 is estimated to be about 65 nm. The sizes of these gap spaces between nano-particles on the $CaCO_3$ microcapsule were accord with the results of nitrogen sorption measurements.

3.2. *Preparation of $CaCO_3$ microcapsules encapsulating proteins*

We produced $CaCO_3$ microcapsules encapsulating some biomacromolecules by the analogous method to silica microcapsules [16]. $CaCO_3$ microcapsules including proteins were prepared by the addition of proteins to the inner water phase. When proteins such as bovine serum albumin were mixed with the aqueous solution of K_2CO_3 used for the inner water phase, the solutions became clouded immediately. The high basicity (pH > 13) of the K_2CO_3 solution probably denatured the proteins and caused them to become insoluble. As the aqueous solution of $(NH_4)_2CO_3$ is less basic (pH ~9.5), the denaturation

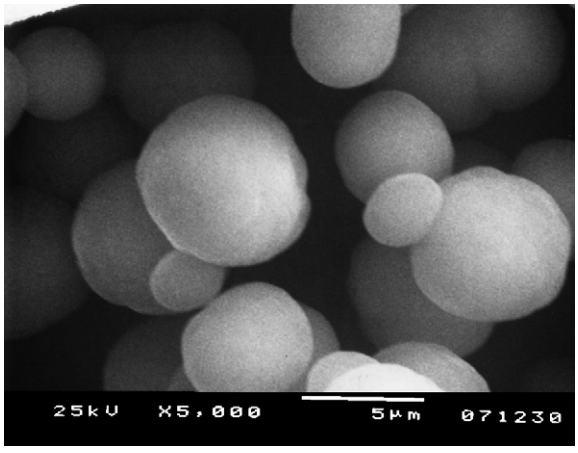

Fig. 7. SEM image of $CaCO_3$ microcapsule encapsulating BSA (CC-BSA).

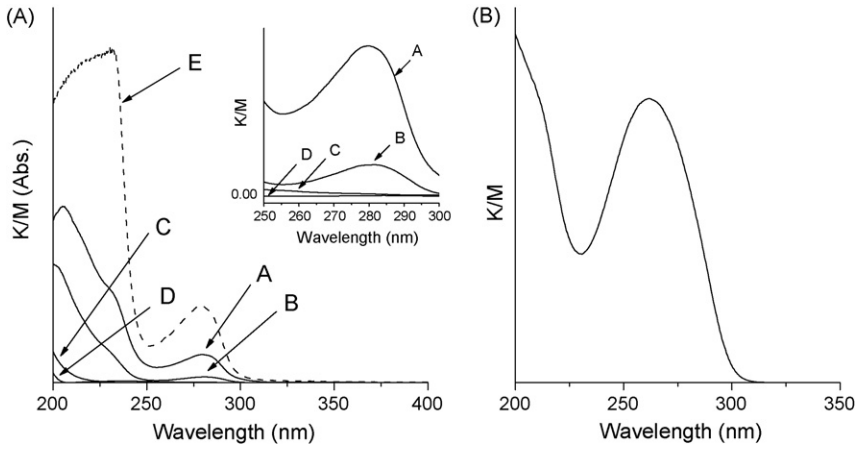

Fig. 8. (A) Diffuse reflectance UV spectrum of $CaCO_3$ microcapsules encapsulating BSA (CC-BSA: A), ovalbumin (CC-Oval: B), papain (CC-Papa: C), and lysozyme (CC-Lyso: D), and UV spectrum of BSA (E). In the inset, an extended figure (from 250 to 300 nm) is shown. (B) DR-UV spectrum of $CaCO_3$ microcapsule encapsulating duplex DNA (CC-DNA).

of proteins will be avoided. No change of the solution occurred after the addition of all proteins into the $(NH_4)_2CO_3$ solution we employed. Therefore, we used $(NH_4)_2CO_3$ as the carbonate salt of the inner water phase in the cases of biomolecule encapsulation. When 0.5 g of BSA was mixed in the inner water phase, BSA was successfully encapsulated into $CaCO_3$ microcapsules. The SEM image of this $CaCO_3$ microcapsule encapsulating BSA is illustrated in Fig. 7. Spherical particles ranging in size from 2 to 10 μm were obtained. The diffuse reflectance ultraviolet (DR-UV) spectrum of this $CaCO_3$ microcapsule including BSA clearly had the characteristic absorption of BSA around 280 nm in the particles as shown in Fig. 8(A).

We applied this direct encapsulation process to other proteins such as ovalbumin, papain and lysozyme. Fig. 8(A) compares all DR-UV spectra of $CaCO_3$ microcapsules encapsulating proteins above listed. The encapsulation profiles of these microcapsules are summarized in Table 2. Although the Kubelka–Munk functions of DR-UV spectra were not so quantitative, the amounts of proteins included in the microcapsules increased with the molecular weights of the proteins. While BSA as the largest protein (66 kDa) in our experiment was evidently included in $CaCO_3$ microcapsule, no UV absorption of lysozyme as the smallest protein (14 kDa) was detected in the corresponding microcapsule (line D of Fig. 8(A)). The results of TGA analyses shown in Table 2 also indicated that the contents of proteins in $CaCO_3$ microcapsules strongly depended on their molecular weight. According to the TGA analysis calculation, BSA was effectively introduced into $CaCO_3$ microcapsule particles, and the efficiency of encapsulation was estimated to be over 90%. This efficiency was higher than those of the encapsulation into silica microcapsules [16]. Ovalbumin (43 kDa) was modestly loaded into the $CaCO_3$ microcapsule particles. (The efficiency was approximately 36%.) On the other hand, papain (21 kDa) as a smaller protein was scarcely encapsulated, and no inclusion of lysozyme into $CaCO_3$ microcapsule was confirmed even in TGA result. In our previous paper on the direct encapsulation of biomacromolecules into silica microcapsule, proteins are partially encapsulated into the silica microcapsules [16]. In another paper, we reported that when some water-soluble polymers were mixed in sodium silicate solution as the inner water phase, these polymers were not encapsulated in the silica microcapsules but instead formed the macropores in the shell wall of silica microcapsules [38]. Even in the case of $CaCO_3$ microcapsules, the considerable amounts of proteins were not encapsulated into the microcapsules. No inclusion of lysozyme into $CaCO_3$ microcapsule was probably caused by the rapid diffusion of lysozyme from the inner water phase to outer one. It is thought that the diffusion rate of proteins is proportional to both their molecu-

Table 2
The profiles of $CaCO_3$ microcapsules encapsulating biomacromolecules

Sample	Biomacromolecules (g)	Mw (Da)[a]	Molecular dimension (nm^3)[a]	Weight loss (%)[b]	Yield (g)	Efficiency (%)[c]
VC–NH–Cl	–	–	–	1.676	9.764	–
CC-BSA	BSA (0.5)	66,400	5.0 × 7.0 × 7.0	6.151	10.340	92.6
CC-Oval	Ovalbumin (0.5)	43,000	4.0 × 5.0 × 7.0	3.469	10.025	36.0
CC-Papa	Papain (0.5)	20,700	3.6	1.935	10.212	5.2
CC-Lyso	Lysozyme (0.5)	14,388	1.9 × 2.5 × 4.3	1.679	8.935	<0.01
CC-DNA	DNA (0.1)	[d]	N/A	1.823	8.984	13.2

[a] Molecular weight and size of proteins are from Ref. [39].
[b] Weight loss from 150 to 600 °C by TGA.
[c] Encapsulation efficiency was estimated from the yields of microcapsules and the measured weight losses of samples after the deduction of weight loss of vacant $CaCO_3$ microcapsule.
[d] 460–14,000 bp.

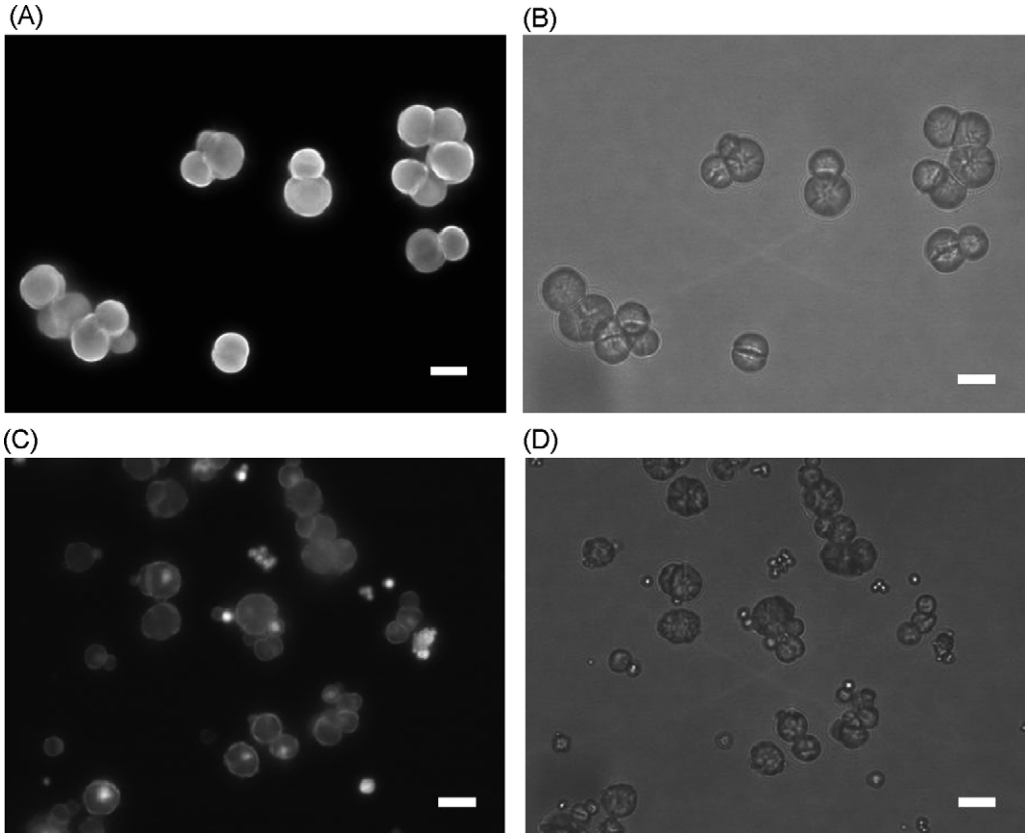

Fig. 9. Fluorescent microscope and photomicroscope images of $CaCO_3$ microcapsules encapsulating BSA with fluorescein (A and B) and BSA-impregnated $CaCO_3$ microcapsules encapsulating with fluorescein (C and D). Length of bar is 10 μm.

lar weight and molecular dimension size listed in Table 2. The encapsulation efficiencies of proteins are well consistent with the molecular weight and molecular size as shown in Table 2.

The $CaCO_3$ microcapsules prepared by the interfacial reaction method tightly included proteins into the microcapsule particles. The proteins thus encapsulated were hardly liberated into aqueous solution. For example, when the $CaCO_3$ microcapsule encapsulating BSA (CC-BSA) was immersed in deionized water, no UV absorption at 280 nm was observed in the supernatant solution. The similar observations have been seen in the cases of silica microcapsule [16] and calcium phosphate particles [26] prepared by the interfacial reaction method. The procedures of the encapsulation of BSA into $CaCO_3$ microcapsule were analyzed by fluorescence microscopy observation. For this experiment, 1% of fluorescein conjugated albumin was added to raw BSA. The images of the microscope observation are summarized in Fig. 9. Pictures A and B in Fig. 9 are fluorescent microscope and photo-microscope images of $CaCO_3$ microcapsules encapsulating BSA with fluorescein at the same place, respectively. The entire parts of all $CaCO_3$ microcapsule particles emitted light uniformly as shown in Fig. 9(A) to reveal the uniform encapsulation of BSA into the $CaCO_3$ microcapsules. Fig. 9(C) and (D) illustrated $CaCO_3$ microcapsule particles, which were prepared by the impregnation

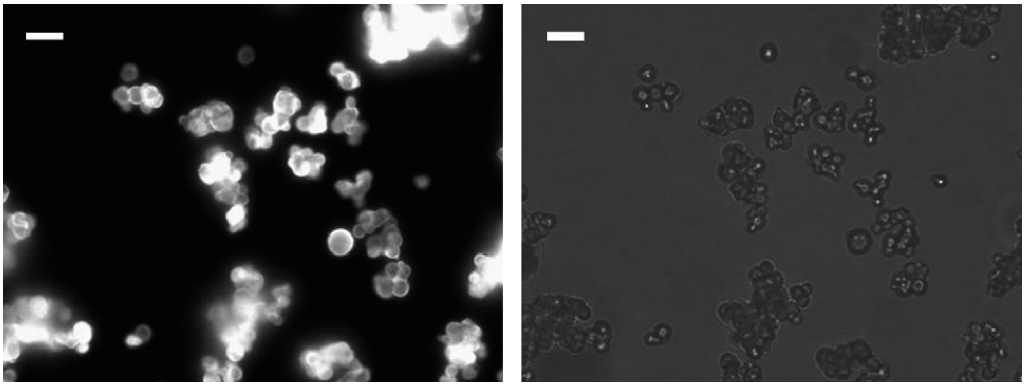

Fig. 10. (A) Fluorescent microscope and (B) photomicroscope images of $CaCO_3$ microcapsules encapsulating duplex DNA with ethidium bromide. Length of bar is 10 μm.

of BSA into VC–NH–Cl as vacant $CaCO_3$ microcapsule. In these BSA "impregnated" $CaCO_3$ microcapsules, only some particles were strongly luminous and other particles were slightly bright (Fig. 9(C)). Thus, BSA was not distributed equally to $CaCO_3$ particles in these samples. Therefore, it was confirmed that the direct encapsulation of BSA by the interfacial reaction method was effective to include BSA homogeneously.

3.3. Preparation of $CaCO_3$ microcapsules encapsulating duplex DNA

Duplex DNA was also encapsulated into $CaCO_3$ microcapsule by the analogous procedure to proteins. We used a deoxyribonucleic acid sodium salt from salmon spermary (from 460 to 14,000 bp) for this experiment. As the solubility of DNA we employed in this research to water was considerably lower than proteins, only 0.1 g of DNA was used for the direct encapsulation process using the interfacial reaction method. Fig. 8(B) is the DR-UV spectrum of $CaCO_3$ microcapsule encapsulating duplex DNA. The characteristic UV absorption of DNA at 260 nm was clearly observed. Without the dissolution of $CaCO_3$ particles, this duplex DNA included in $CaCO_3$ microcapsules was not released into the aqueous solution similar to BSA. The efficiency of the encapsulation was estimated to be about 13% as shown in Table 2. The inclusion manner of DNA in the $CaCO_3$ microcapsule was also analyzed by the fluorescence microscope observation. Ethidium bromide was impregnated to the $CaCO_3$ microcapsule with duplex DNA. After thorough water washing, fluorescence microscope observation was performed. Fig. 10 is the fluorescence microscope and photo-microscope images of the same observation field. All particles of $CaCO_3$ microcapsule produced fluorescence. Even in the case of duplex DNA, the effective encapsulation and the homogeneous distribution of DNA in the $CaCO_3$ microcapsule were achieved.

4. Conclusions

We reported in this paper that $CaCO_3$ microcapsules were effectively obtained by the interfacial reaction method using both carbonate salts such as K_2CO_3 and $(NH_4)_2CO_3$ in the inner water phase and calcium salts such as $CaCl_2$ in the outer water phase. When some biomacromolecules such as BSA and duplex DNA were mixed in the inner water phase, they were encapsulated directly into the $CaCO_3$ microcapsules. The efficiency of the encapsulation of proteins strongly depended on their molecular weight. While BSA with higher molecular weight was included effectively, no encapsulation of lysozyme with lower molecular weight was observed. Biomacromolecules thus encapsulated scarcely eliminated without the fracture of the microcapsule particles. Our encapsulation method reported here is quite simple and not time-consuming. This procedure will be utilized in various fabrications of bio-related materials.

Acknowledgment

This work was supported by "Secure and Healthy Livestock Farming Project" of the Ministry of Agriculture, Forestry and Fisheries of Japanese Government.

References

[1] S. Giri, B.G. Trewyn, V.S.Y. Lin, Mesoporous silica nanomaterial-based biotechnological and biomedical delivery systems, Nanomedicine 2 (2007) 99–111.
[2] S. Jin, K.M. Ye, Nanoparticle-mediated drug delivery and gene therapy, Biotechnol. Prog. 23 (2007) 32–41.
[3] J.M. de la Fuente, C.C. Berry, M.O. Riehle, A.S.G. Curtis, Nanoparticle targeting at cells, Langmuir 22 (2006) 3286–3293.
[4] C.C. Berry, Possible exploitation of magnetic nanoparticle–cell interaction for biomedical applications, J. Mater. Chem. 15 (2005) 543–547.
[5] F.Y. Cheng, C.H. Su, Y.S. Yang, C.S. Yeh, C.Y. Tsai, C.L. Wu, M.T. Wu, D.B. Shieh, Characterization of aqueous dispersions of Fe_3O_4 nanoparticles and their biomedical applications, Biomaterials 26 (2005) 729–738.
[6] T. Coradin, M. Boissiere, J. Livage, Sol–gel chemistry in medicinal science, Curr. Med. Chem. 13 (2006) 99–108.
[7] P.X. Zhi, H.Z. Qing, Q.L. Gao, B.Y. Ai, Inorganic nanoparticles as carriers for efficient cellular delivery, Chem. Eng. Sci. 61 (2006) 1027–1040.
[8] H. Hillebrenner, F. Buyukserin, J.D. Stewart, C.R. Martin, Template synthesized nanotubes for biomedical delivery applications, Nanomedicine 1 (2006) 39–50.
[9] D.W. Yu, T.T. Fukuda, S. Kuroda, K. Tanizawa, A. Kondo, M. Ueda, T. Yamada, H. Tada, M. Seno, Engineered bio-nanocapsules, the selective vector for drug delivery system, IUBMB Life 58 (2006) 1–6.
[10] Y. Ding, Y. Hu, L.Y. Zhang, Y. Chen, X.Q. Jiang, Synthesis and magnetic properties of biocompatible hybrid hollow spheres, Biomacromolecules 7 (2006) 1766–1772.
[11] N.E. Botterhuis, Q.Y. Sun, P.C.M.M. Magusin, R.A. van Santen, N.A.J.M. Sommerdijk, Hollow silica spheres with an ordered pore structure and their application in controlled release studies, Chem.-Eur. J. 12 (2006) 1448–1456.
[12] M. Vallet-Regi, D. Arcos, Nanostructured hybrid materials for bone tissue regeneration, Curr. Nanosci. 2 (2006) 179–189.
[13] R.Y. Kannan, H.J. Salacinski, P.E. Butler, A.M. Seifalian, Polyhedral oligomeric silsesquioxane nanocomposites: the next generation material for biomedical applications, Acc. Chem. Res. 38 (2005) 879–884.
[14] F. Balas, M. Manzano, P. Horcajada, M. Vallet-Regi, Confinement and controlled release of bisphosphonates on ordered mesoporous silica-based materials, J. Am. Chem. Soc. 128 (2006) 8116–8117.
[15] M. Fujiwara, K. Shiokawa, Y. Tanaka, Y. Nakahara, Preparation and formation mechanism of silica microcapsules (hollow sphere) by water/oil/water interfacial reaction, Chem. Mater. 16 (2004) 5420–5426.
[16] M. Fujiwara, K. Shiokawa, K. Hayashi, K. Morigaki, Y. Nakahara, Direct encapsulation of BSA and DNA into silica microcapsules (hollow spheres), J. Biomed. Mater. Res. A 81 (2007) 103–112.
[17] J.M. Xue, C.H. Tan, D. Lukito, Biodegradable polymer–silica xerogel composite microspheres for controlled release of gentamicin, J. Biomed. Mater. Res. B 78 (2006) 417–422.
[18] T. Czuryszkiewicz, J. Ahvenlammi, P. Kortesuo, M. Ahola, F. Kleitz, M. Jokinen, M. Linden, J.B. Rosenholm, Drug release from biodegradable silica fibers, J. Non-Cryst. Solids 306 (2002) 1–10.
[19] M. Kursawe, W. Glaubitt, A. Thierauf, Biodegradable silica fibers from sols, J. Sol–Gel Sci. Technol. 13 (1998) 267–271.
[20] D. Luo, W.M. Saltzman, Nonviral gene delivery—thinking of silica, Gene Ther. 13 (2006) 585–586.
[21] D.J. Bharali, I. Klejbor, E.K. Stachowiak, P. Dutta, I. Roy, N. Kaur, E.J. Bergey, P.N. Prasad, M.K. Stachowiak, Organically modified silica nanoparticles: a nonviral vector for in vivo gene delivery and expression in the brain, Proc. Natl. Acad. Sci. U.S.A. 102 (2005) 11539–11544.

[22] I. Roy, T.Y. Ohulchanskyy, D.J. Bharali, H.E. Pudavar, R.A. Mistretta, N. Kaur, P.N. Prasad, Optical tracking of organically modified silica nanoparticles as DNA carriers: a nonviral, nanomedicine approach for gene delivery, Proc. Natl. Acad. Sci. U.S.A. 102 (2005) 279–284.
[23] S. Nayar, M.K. Sinha, D. Basu, A. Sinha, Synthesis and sintering of biomimetic hydroxyapatite nanoparticles for biomedical applications, J. Mater. Sci.: Mater. Med. 17 (2006) 1063–1068.
[24] W. Tjandra, P. Ravi, J. Yao, K.C. Tam, Synthesis of hollow spherical calcium phosphate nanoparticles using polymeric nanotemplates, Nanotechnology 17 (2006) 5988–5994.
[25] M. Vallet-Regi, J.M. Gonzalez-Calbet, Calcium phosphates as substitution of bone tissues, Prog. Solid State Chem. 32 (2004) 1–31.
[26] M. Fujiwara, K. Shiokawa, K. Morigaki, Y. Tatsu, Y. Nakahara, Calcium phosphate composite materials including inorganic powders, BSA or duplex DNA prepared by W/O/W interfacial reaction method, Mater. Sci. Eng. C 28 (2008) 280–288.
[27] Y. Nakahara, M. Mizuguchi, K. Miyata, Effects of surfactants on $CaCO_3$ spheres prepared by interfacial reaction method, J. Colloid Interface Sci. 68 (1979) 401–407.
[28] T. Kato, A. Sugawara, N. Hosoda, Calcium carbonate–organic hybrid materials, Adv. Mater. 14 (2002) 869–877.
[29] D. Walsh, S. Mann, Fabrication of hollow porous shells of calcium-carbonate from self-organizing media, Nature 377 (1995) 320–323.
[30] Y.S. Han, G. Hadiko, M. Fuji, M. Takahashi, A novel approach to synthesize hollow calcium carbonate particles, Chem. Lett. 34 (2005) 152–153.
[31] G. Hadiko, Y.S. Han, M. Fuji, M. Takahashi, Synthesis of hollow calcium carbonate particles by the bubble templating method, Mater. Lett. 59 (2005) 2519–2522.
[32] Q. Yu, H.D. Ou, R.Q. Song, A.W. Xu, The effect of polyacrylamide on the crystallization of calcium carbonate: synthesis of aragonite single-crystal nanorods and hollow vatarite hexagons, J. Cryst. Growth 286 (2006) 178–183.
[33] N. Loges, K. Graf, L. Nasdala, W. Tremel, Probing cooperative interactions of tailor-made nucleation surfaces and macromolecules: a bioinspired route to hollow micrometer-sized calcium carbonate particles, Langmuir 22 (2006) 3073–3080.
[34] A.I. Petrov, D.V. Volodkin, G.B. Sukhorukov, Protein-calcium carbonate coprecipitation: a tool for protein encapsulation, Biotechnol. Prog. 21 (2005) 918–925.
[35] D.V. Volodkin, N.I. Larionova, G.B. Sukhorukov, Protein encapsulation via porous $CaCO_3$ microparticles templating, Biomacromolecules 5 (2004) 1962–1972.
[36] G.B. Sukhorukov, D.V. Volodkin, A.M. Gunther, A.I. Petrov, D.B. Shenoy, H. Mohwald, Porous calcium carbonate microparticles as templates for encapsulation of bioactive compounds, J. Mater. Chem. 14 (2004) 2073–2081.
[37] K.S.W. Sing, D.H. Everett, R.A.W. Haul, L. Moscou, R.A. Pierotti, J. Rouquérol, T. Siemieniewska, Pure Appl. Chem. 57 (1985) 603–619.
[38] M. Fujiwara, K. Shiokawa, I. Sakakura, Y. Nakahara, Silica hollow spheres with nano-macroholes like diatomaceous earth, Nano Lett. 6 (2006) 2925–2928.
[39] M. Hartmann, Ordered mesoporous materials for bioadsorption and biocatalysis, Chem. Mater. 17 (2005) 4577–4593.